ElectroPad: Extending Gamepad Haptics for Hand Movements in Video Games with Electrotactile Feedback

Wenxuan Li
Hunan University
Changsha, China
Institute of Software, Chinese Academy of Sciences
Beijing, China
liwenxuan385@hnu.edu.cn

Hongnan Lin*
Institute of Software, Chinese Academy of Sciences
Beijing, China
linhongnan@iscas.ac.cn

Shengsheng Jiang
Institute of Software, Chinese Academy of Sciences
Beijing, China
haofan2@emails.bjut.edu.cn

Jiaqi Zheng
Hunan University
Changsha, China
zhengjiaqi@hnu.edu.cn

Xinyi Gao
Hunan university
Changsha, China
xinyigao@hnu.edu.cn

Hechuan Zhang
Institute of Software, Chinese Academy of Sciences
Beijing, China
zhanghechuan21@mails.ucas.ac.cn

Luyao Shen
Institute of Software, Chinese Academy of Sciences
Beijing, China
The Hong Kong University of Science and Technology (Guangzhou)
Guangzhou, China
lshen595@connect.hkust-gz.edu.cn

Teng Han
Institute of Software, Chinese Academy of Sciences
Beijing, China
hanteng1021@gmail.com

Feng Tian
Institute of software, Chinese Academy of Sciences
Beijing, China
tianfeng@iscas.ac.cn

Wei Wang*
Hunan University
Changsha, China
wangwei1125@hnu.edu.cn

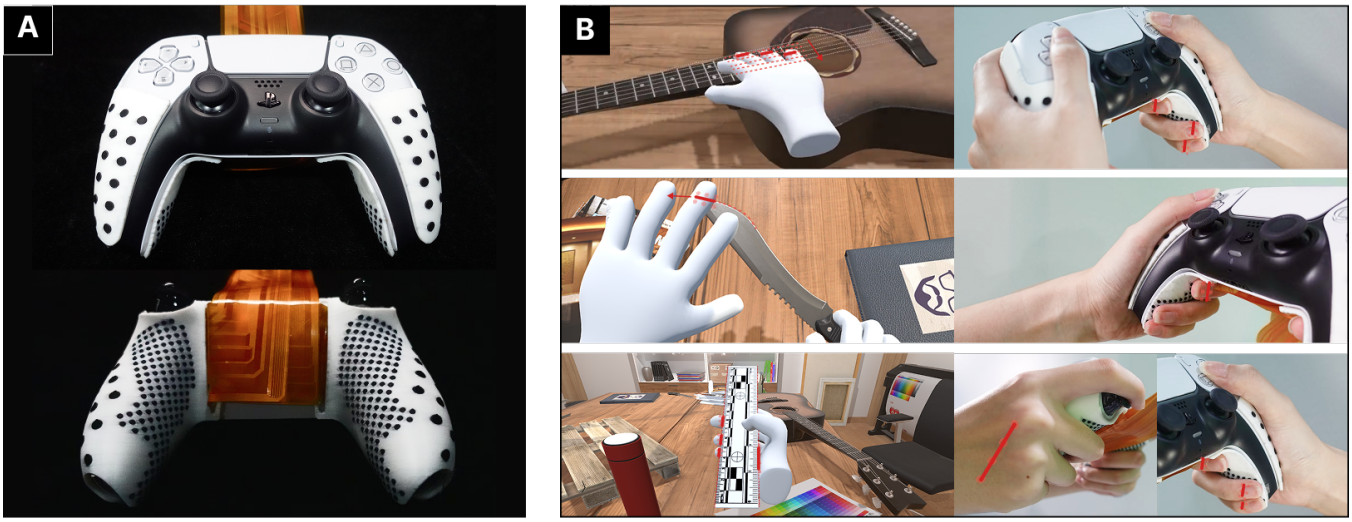


Figure 1: A. Photos of the ElectroPad. B. ElectroPad supports hand-movement scenarios through providing detailed haptic cues by independently driving a dense array of electrodes mapped to hand regions in contact with virtual objects.

*Co-corresponding author.

This work is licensed under a Creative Commons Attribution 4.0 International License.

UIST '26, Detroit, MI, USA

© 2026 Copyright held by the owner/author(s).

ACM ISBN 979-8-4007-2856-3/26/11
https://doi.org/10.1145/3830398.3830656

Abstract

Gamepads are among the most widely used haptic devices, yet their haptic feedback remains limited in supporting hand-movement scenarios in video games that require precise tactile sensations at specific hand locations. Electrotactile feedback offers a promising alternative, providing high-resolution, precisely mapped stimulation that can be seamlessly integrated onto controller surfaces. We present ElectroPad, an electrotactile gamepad cover embedding 190 electrodes per handle, delivering rich texture and shape feedback to hand regions in contact with virtual objects. Two user studies demonstrate that our system reliably conveys tactile cues, achieving mid-to-high levels of realism, while significantly enhancing enjoyment and immersion compared to visual-only conditions. Participants also expressed strong willingness to adopt the system and offered concrete suggestions for refinement. These findings highlight electrotactile stimulation as a powerful complement to gamepad haptics, expanding the design space for game interactions and enabling more expressive user experiences.

CCS Concepts

• **Human-centered computing → Haptic devices**.

Keywords

Electrotactile, Gamepad, Haptic Feedback, Hand-Movement Interaction

ACM Reference Format:

Wenxuan Li, Hongnan Lin, Shengsheng Jiang, Jiaqi Zheng, Xinyi Gao, Hechuan Zhang, Luyao Shen, Teng Han, Feng Tian, and Wei Wang. 2026. ElectroPad: Extending Gamepad Haptics for Hand Movements in Video Games with Electrotactile Feedback. In *The 39th Annual ACM Symposium on User Interface Software and Technology (UIST '26), November 02–05, 2026, Detroit, MI, USA.* ACM, New York, NY, USA, 14 pages. https://doi.org/10.1145/3830398.3830656

1 Introduction

Hand movements in video games are prevalent as forms of virtual hand–object interactions across diverse game contexts, such as weapon manipulation in FPS games, object interaction in puzzle games, and environment exploration in open-world settings. Such object-exploring hand movements have been categorized into a set of Exploratory Procedures (EPs) [21], and are typically realized in games through cutscene animations, triggered interactions, and real-time interactive animations, largely driven by pre-authored animation assets. These hand movements play an essential role in engaging players, particularly in first-person settings, and haptic feedback has been widely adopted to enhance such experiences.

As one of the most common haptic interfaces in video games, current gamepads support EPs primarily through vibration for overall hand and force feedback on fingers [19, 32]. Vibration is used to simulate impacts, roughness, resistance and weight distribution associated with handheld objects [19, 32, 57], such as the recoil of a weapon, the friction during page flipping, the resistance when turning a lock, or imbalance between the two hands when shaking a box. In contrast, trigger-based force feedback conveys compliance and resistance [19, 32], for example when drawing a bow or pulling a gun trigger. However, despite these capabilities, both whole-hand vibration and finger-based force remain limited in supporting EPs requiring precise tactile sensations at specific hand locations, including lateral motion (LM) for perceiving surface relief, contour following (CF) for exact shape, and enclosure (EN) for global shape. Specifically, vibration generated by a gamepad's two motors cannot provide fine-grained feedback over small spatial regions, while trigger-based force feedback is restricted to specific fingers, and neither method can convey detailed tactile patterns. For instance, the engraving marks on fingertips when stroking a wall, the sharp edge of a blade brushing against a finger, or the corners of an object sliding across the hand remain difficult to render.

Electrotactile feedback, which can render detailed tactile patterns via surface electrodes, offers a solution to the limitations of conventional vibration and force feedback on gamepads. Building on this potential, we developed ElectroPad, a pair of 2 mm-thick electrotactile controller covers exploring high-density electrotactile integration on existing handheld surfaces. The electrode layout is informed by diverse hand sizes and tactile characteristics, integrating 145 small electrodes (2 mm diameter, 3.5 mm spacing) for the fingers and 45 larger electrodes (4 mm diameter, 10 mm spacing) for the palm, primarily distributed over frequently contacted regions. Each cover combines a dual-material 3D-printed shell embedding 190 electrodes with a flexible printed circuit (FPC), enabling high-density electrodes on highly curved surfaces. During virtual hand–object interaction, contact points detected by probes on a virtual hand are mapped to corresponding physical electrodes on the gamepad. This mapping is individualized based on users' grips, and each electrode can be driven independently. This enables precise, hand-surface-mapped stimulation for three EPs - LM, CF and EN - in game, allowing users to feel surface reliefs through LM, sense edges via CF, and perceive overall shape through EN.

We conducted two user studies to evaluate our system. Study 1 examined haptic perception and haptic experience, with participants experiencing electrotactile feedback of exploring various geometric objects through diverse hand contact across three EP scenarios. The results show that our approach can deliver tactile sensations across multiple localized hand regions, with particularly reliable perception exceeding 90% at the fingertips, thenar eminence, and MCP joints, achieves a moderate-to-high level of perceived realism, and demonstrates the potential to support discriminable object features, while providing guidance for the design of object and hand-contact settings. Study 2 evaluated usability in game-like scenarios, where participants interacted with items through exploratory movements, revealing significant improvements in enjoyment, immersion, and adoption intent with electrotactile feedback, along with insights for future applications.

Our work makes the following contributions: (1) A novel prototype system that explores high-density electrotactile integration on existing handheld surfaces, supporting diverse hand sizes and grips by design, enabling high-density electrodes on highly curved surfaces in fabrication, and supporting efficient, independently addressable electrode control at scale for driving. (2) A method that allows the gamepad to provide fine-grained tactile feedback associated with object-exploring hand movements, via a personalized mapping between virtual probes and physical electrodes. (3) User-validated applications and design guidelines, demonstrating the

potential of electrotactile feedback to enhance gameplay and enable more expressive interactions.

2 Related Work

2.1 Haptic Experience on Gamepads

Gamepads are one of the most common input devices for two-handed, ergonomic control, featuring buttons, joysticks, and triggers for intuitive navigation and interaction.

To enhance immersion, haptic feedback has been widely integrated into gamepads. Vibration is the most prevalent form of gamepad haptics [32, 42] and is supported by most mainstream gamepads. Microsoft Xbox controllers use Eccentric Rotating Mass (ERM) actuators, while Nintendo Switch controllers employ Linear Resonant Actuators (LRAs) in their handles [4, 42]. PlayStation 5 DualSense controller utilizes voice-coil motors in each handle [19] and controls vibration via audio signals [4], enabling a broad range of refined sensations, from environmental textures to weapon recoil and shifts in weight distribution [32]. Apart from vibration feedback, gamepads use force feedback, particularly in triggers, to simulate real-world interactions. For example, the PS5 DualSense's adaptive triggers adjust the resistance of the trigger buttons based on the game scenario, allowing for varying levels of resistance depending on the weapon used by the player or simulating different pressure levels for acceleration and braking in racing games [32]. Some research has also explored force feedback on joysticks and buttons to simulate stiffness or object interactions [41, 42]. Thermal feedback has also been investigated for ambient cues or atmosphere creation [27].

However, due to the inherent characteristics and actuation mechanisms, these haptic modalities either deliver overall-hand effects or are confined to a specific location, limiting spatially distributed haptic rendering across the hand. Moreover, they struggle to render fine-grained tactile patterns. These limitations constrain their support for hand movements requiring localized tactile patterns on multiple hand regions, such as LM, CF and EN, which are defined in Lederman and Klatzky's taxonomy of hand exploration [21].

2.2 Localized Haptic Rendering for Hand Movements

Localized haptic cues across the hands play an important role in improving users' perception of virtual object properties during hand-object interaction, which enhances immersion [52] and facilitates interaction and teleoperation in virtual environments [43].

Compared with video game research, VR research has focused more on spatially distributing additional actuators or applying finer haptic modalities to support stroking and grasping interactions. Examples include shape-changing mechanical displays [7, 50, 58], brake mechanisms [5, 59], and physical proxies [49] for rendering object size and shape, as well as electrotactile stimulation [25, 56], ultrasound-based haptics [30], and full-hand distributed vibration [28] for rendering surface patterns or shape cues.

However, although these techniques provide richer support for hand movements, their form factors are often limited to wearable devices [5, 28, 50, 59], desktop installations [30], or custom-designed handheld prototypes [7, 58]. Few solutions are integrated into widely used commercial handheld controllers, such as the gamepad form factor used in our study. This may limit their accessibility and broader adoption in mainstream interactive systems and applications.

Based on these limitations, we explore integrating precise tactile feedback across the large contact surface of a game controller to better support hand movements in video games.

2.3 Electrotactile Stimulation

Electrotactile feedback is a tactile sensation generated by applying electrical current through electrodes on the skin surface [15]. The current flows between the electrodes, with the anode (high voltage) transmitting the current to the cathode (ground), which directly stimulates the sensory nerves in the skin. Electrotactile stimulation can render high-resolution tactile feedback, enabling the display of vibration [60], texture [6], roughness [2], spatial patterns [9, 12], and dynamic interactions [11, 46]. It has also been used to provide pseudo-force feedback such as pressure and traction [31, 33], enabling perception of object attributes like compliance [10] and weight [22], and can even evoke thermal sensations [39]. The combination of electrotactile with force feedback is also used to present 3D shape [44] and softness [45]. To facilitate these diverse applications, several electrotactile platforms [20, 34] have been developed for efficient generation and control of electrotactile feedback. The rich electrotactile sensations have been explored in virtual hand exploration, such as improving perception of tactile features in mixed reality [47], rendering tactile images to feel objects while reaching or hovering [48]. However, their coverage or density may not support some hand-object interactions such as EN in our work. In contrast, our electrotactile on a broader surface enables these multi-region hand-object interactions.

In addition to precise tactile sensations, electrotactile stands out on form factor compared to other methods due to small and thin size, low cost, energy efficiency, and durability, making it highly valuable for various applications. The form factor of electrotactile on hands can generally be categorized into wearable and handheld devices. Wearable devices include thin-film interfaces that adhere directly to the skin, typically fabricated by printing conductive materials onto flexible substrates such as silicone [56], stretchable TPU films [25], coated paper [10, 11] or tattoo paper [55]. Other wearable form factors—such as finger caps and gloves—integrate FPCs into structures like finger cots [25, 26, 36], bandages [1], or glove shells [1, 38]. There are also textile electrodes adopting a multi-layer woven structure that separates conductive weft and warp electrodes with non-conductive yarns [24]. Handheld devices, in contrast, comprise portable objects with embedded electrode arrays, including cylindrical grips [13], smartphones [8, 17, 18, 46], touchscreens [14, 23] and mice [23]. Most handheld prototypes embed PCBs, FPCs, or inkjet-printed films into designated regions of the device [8, 13, 14, 17, 18, 23, 46], and 3D printing has also been used to integrate electrode arrays onto product surfaces [8]. Most stimulation is focused on the fingertip of the index finger, followed by other fingers and the palm. The highest reported electrode density reaches up to 76 dots/cm² [25]. On the fingers, electrode sizes typically range from 1 to 3 mm, with spacing between 2 and 5 mm [10, 13, 16–18, 25, 35, 51, 55, 56]. On the palm, electrode sizes range from 3 to 11 mm, with spacing between 2.54 and 13

mm [1, 13, 17, 25, 56]. These electrodes are typically embedded on flat surfaces [8, 17, 18], edges [46], or simple curved geometries [8, 13] with relatively low electrode density. However, there has been very limited research on embedding high-density electrode arrays onto rigid, irregularly shaped existing product surfaces, such as the handle shell used in this study.

Building on the fine-grained tactile rendering capability and compact form factor of electrotactile stimulation, we adopt high-density electrotactile feedback on the broad surface of a gamepad, to support tactile perception for more hand movement scenarios. To achieve this, we combine FPCs with a 3D-printed outer shell, enabling both a high-density wiring layout and seamless conformity between the electrodes and the irregularly shaped gamepad surface.

3 Design and Implementation of ElectroPad

As shown in Figure 2, ElectroPad consists of three layers: the outer 3D-printed shell with embedded electrodes, the inner FPC for electrode driving, and the two layers are connected by anisotropic conductive tape in the middle.

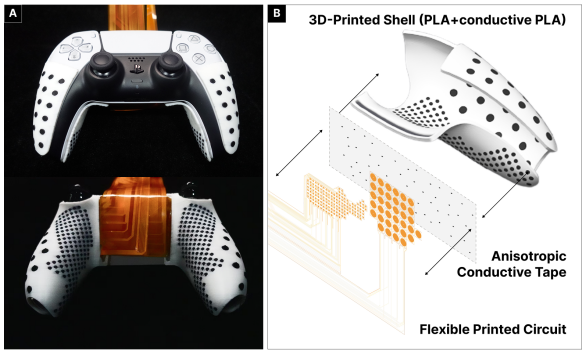


Figure 2: A, the photo of ElectroPad. B, the structure of ElectroPad.

3.1 Determining the Area for Electrotactile

To ensure the electrode placement is both generalizable and usable, we firstly conducted a contact area collection study to analyze how users with different hand sizes grip gamepads, identifying typical contact regions on the controller and corresponding hand areas to guide electrode placement, excluding the thumb and index finger due to their frequent movements during gameplay.

3.1.1 Participants. Nine experienced gamepad users (6 males, 3 females, aged 21–32) were recruited. As hand length was observed to be an important factor influencing the contact area on the gamepad, participants were selected with hand lengths representative of common adult ranges defined in GB/T 16252–2023: 175–205 mm for males (approximately 86.4% of the male population) and 155–175 mm for females (approximately 74.4% of the female population). All participants reported no hand-related medical conditions.

3.1.2 Materials. The experiment used a PS5 DualSense controller. Paper tape was applied to both grips to fully conform to the controller's shape. To facilitate flattening of the curved surfaces, we divided the right grip into four parts. Red ink captured contact areas on the controller where users gripped it, while blue acrylic paint marked corresponding areas on participants' hands.

3.1.3 Procedure. Before the experiment began, participants were briefed on the study and provided informed consent. Blue paint was applied to the paper covering the left grip of the controller, while red ink was applied to the participant's right hand. Participants were then instructed to hold the controller as if actively playing a game, imagining typical in-game interactions rather than maintaining a static grip. After naturally moving their hands to mimic gameplay actions for 30 s, the blue paint marked the contact areas on the left hand, while the red ink left imprints on the right grip. Finally, participants' left hands were positioned as specified, and the paper tapes from the right grip were removed and flattened. All results were documented with photographs.

3.1.4 Results.

Controller Contact Areas. Controller imprints were scanned and processed to enhance clarity. Excluding thumb and index finger areas, contact regions were outlined in the four predefined sections (Figure 3). Measured areas were: 1955.94 mm² (42.2 × 73.8 mm), 1534.47 mm² (25.2 × 77.4 mm), 831.43 mm² (43.5 × 26.9 mm), and 1620.26 mm² (52.4 × 50.9 mm), totaling 5942.10 mm².

Hand Contact Areas. Hand imprints were scanned and processed similarly. Excluding thumb and index finger areas, contact was concentrated in the thenar eminence, hypothenar, bases of the four fingers (MCP joints), and pads of the middle, ring, and little fingers. The palm center and palm lines showed relatively weaker contact. Total contact area was 5595.18 mm², smaller than the controller's, reflecting variation in finger contact patterns across users. Hence, more areas were defined on the controller to accommodate these differences.

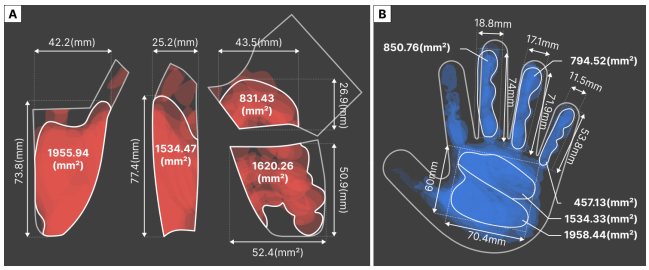


Figure 3: Contact Area Results. A, Controller Contact Areas. B, Hand Contact Areas.

3.2 Electrode Arrangement

To ensure sufficient feedback precision while minimizing the total number of electrodes for simplifying hardware control, we set different electrode spacing for palm and finger regions based on their electrotactile two-point discrimination.

Prior work reports discrimination thresholds of 1.5 mm at the fingertip, 3 mm on other finger regions, and 8 mm on the palm [13], with electrotactile thresholds on the fingers ranging from 2–4

mm [16]. Existing designs typically use electrode sizes of 1.2–3 mm for fingers and 3–11 mm for palm, with spacings of 2–5 mm and 2.54–13 mm respectively [1, 10, 13, 17, 18, 25, 55, 56]. The highest reported electrode density reaches 76 dots/cm² [25].

Based on these findings, we set electrode spacing to 3.5 mm for the fingers and 10 mm for the palm, covering the identified contact areas (Section 3.1). To ensure manufacturability, a minimum edge-to-edge spacing of 1.5 mm was enforced to avoid conductive shorting during 3D printing.

The final design uses 2 mm diameter electrodes with 3.5 mm spacing on the fingers and 4 mm diameter electrodes with 10 mm spacing on the palm, totaling 190 electrodes per hand (380 for both hands).

Considering that variations in hand pressure during controller gripping may affect electrotactile two-point discrimination, we conducted a verification study with 10 participants following Kajimoto et al. [16]. Adjacent electrodes were stimulated quasi-simultaneously, and participants reported perceiving one point, two points, or a short line. Across all palm and finger regions, two-point responses remained below 0.25, with perceptions predominantly reported as a single point or short line. These results suggest that the chosen electrode spacing remains within perceptual limits during controller use.

3.3 Fabrication

We designed a handle shell integrating the electrodes using 3D modeling software, consisting of left and right shells conforming to PS5 grips with button openings for operation. Electrodes are positioned in the contact regions identified in the area collection (see Section 3.1), with sizes and spacings set to 4 mm diameter and 10 mm spacing for the palm, and 2 mm diameter and 3.5 mm spacing for the fingers. A 6 mm buffer zone was added between palm and finger regions to reduce occasional tingling along the fingers. Each electrode protrudes 0.1 mm to ensure reliable skin contact, and all electrodes share a consistent projection direction for smooth transitions and improved aesthetics.

The outer shell was fabricated using dual-material FDM printing, with conductive PLA ($\approx 2\ \Omega\cdot$cm) for electrodes and non-conductive PLA for the rest. Printing was performed on a Bambu Lab H2D with a 0.2 mm nozzle at 220°C.

The inner FPC layer adopts a dual-layer fabrication and hollow structural design, enabling dense circuitry for independent control of each electrode while conforming to the gamepad's curved surface (Figure 2).

3.4 Control Circuit

As shown in Figure 4, the control circuit consists of a programmable high-voltage power supply, a Communication Centralization & Timing Control module, a high-voltage switching module, a PC running stimulation pattern programs, and the ElectroPad with its electrode array.

The programmable high-voltage source was implemented using a Keithley 2470 Source Meter, which supplied high voltage with limited current. A Unity program running on the PC generated stimulation patterns in real time and transmitted them to the Communication Centralization & Timing Control module via

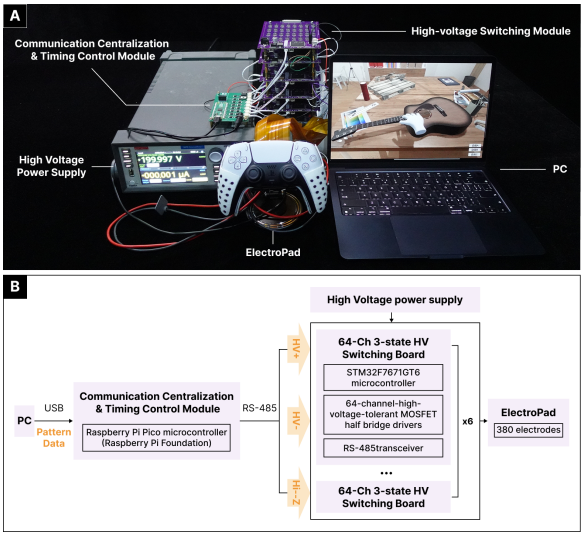


Figure 4: A, control circuit photo. B, the principle of the control circuit.

a serial connection. This module employed a Raspberry Pi Pico microcontroller as the primary control unit. It received pattern information from the PC and relayed commands to the switching boards through an RS-485 communication bus, with a timing precision of $\leq 1\ \mu$s. This enabled dynamic routing of electrode nodes to the high-voltage positive (HV+), high-voltage negative (HV−), or a high-impedance (Hi−Z) floating state. The high-voltage switching module comprised six 64-channel tri-state high-voltage switching boards. Each board integrated an STM32F767IGT6 microcontroller, 64-channel high-voltage-tolerant MOSFET half-bridge drivers, and an RS-485 transceiver. This architecture allowed the boards to execute commands from the Communication Centralization & Timing Control module and dynamically route current across designated electrodes on the controller cover under real-time constraints.

3.5 Stimulation Method

To accommodate diverse grip patterns, we first perform a user-specific mapping to identify actual contact points on the controller and map them onto a virtual hand in Unity (Figure 5), ensuring correspondence with real-world hand regions. Users held the controller naturally while all electrodes are scanned using a calibrated current, starting from 50 μA, to distinguish contact from non-contact without causing discomfort. Each electrode is sequentially activated at high voltage while three surrounding electrodes are grounded, and returned current values are visualized using a viridis colormap to extract palm and finger contact points. The scanning takes about 5 minutes.

Disc-shaped collision probes are then placed on the virtual hand according to the electrode layout, initially covering all identified contact areas—7×7 for each palm, 5×22 for middle fingers, 4×20 for ring fingers, and 3×15 for little fingers. Probes are then retained only if they match actual contact electrodes. Palm probes follow the electrode grid, while finger probes are arranged diagonally at 45° from fingertip to base. Left and right hand finger probes

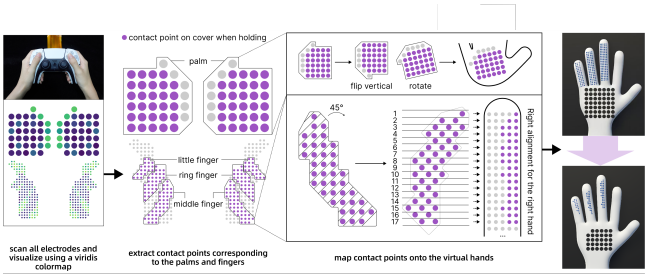


Figure 5: The user-specific mapping process identifying the actual contact points on the controller and mapping them onto the virtual hand in Unity.

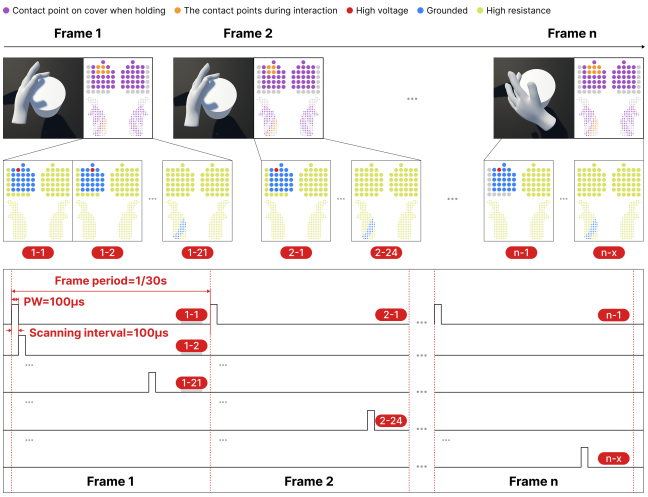


Figure 6: The stimulation information of electrotactile feedback.

are assigned left-to-right and right-to-left, respectively, reflecting natural contact orientation.

During interaction, contact probes between the virtual hand and objects are detected at each probe level (Figure 6) and transmitted to the hardware at 30 fps. Electrodes corresponding to contacted probes are then activated.

Within the stimulation area, anodal pulses are applied sequentially at 100 μs intervals across all points. During each scan, the target electrode is set to high voltage, other electrodes in the same hand region are grounded, and the remaining electrodes are set to high-impedance to prevent unintended stimulation. Pulse amplitude is individually calibrated, while pulse width is fixed at 100 μs to ensure a clear yet pain-free sensation [15]. The pulse width was not adjusted for different stimulation animation durations.

For safety considerations, several electrodes at the MCP–finger boundary and the outer central thenar region were proactively masked based on prior observations of occasional discomfort or involuntary movements, affecting only 1-2 isolated locations in a few participants. All individually adjusted stimulation amplitudes remained well below the Type BF patient leakage current limit (100 μA) specified in IEC 60601-1, which serves as a conservative safety reference. All procedures received ethics approval, and no adverse events or skin injuries were reported during the user studies.

4 Study 1: Investigating Users' Haptic Perception and Experience

Study 1 investigates users' haptic perception and experience, examining perceptual reliability across hand regions, perceived realism of the feedback, and the capability boundaries for object discrimination, thereby evaluating the proposed system and informing design considerations for potential applications.

RQ1: How does the electrotactile feedback support users' perception across different hand regions under the three EPs?

RQ2: How does the perceived realism of the haptic feedback vary across different object and hand contact conditions under the three EPs?

RQ3: To what extent can the electrotactile feedback enable users to discriminate between objects under different hand contact conditions?

4.1 Study Design

We explored users' haptic perception and experience under three EPs — LM, CF, and EN — by varying two factors: object condition and hand contact condition.

- LM: Texture spacing affects users' ability to perceive surface patterns [29], while different hand regions introduce varying levels of tactile information complexity. Three texture densities (SPARSE, DENSE, SPARSE-TO-DENSE) were selected as object conditions, along with three hand contact conditions (SINGLE-FINGER, MULTI-FINGER, OVERALL-HAND), resulting in 9 scenarios.
- CF: Edge geometries lead to different movement trajectories across the hand, and perception to electrotactile lines may vary across hand regions. Two geometries (STRAIGHT, CURVE) and five hand contact conditions (SINGLE-FINGER, PALM-LATERAL, PALM-VERTICAL, MULTI-FINGER, FINGER-PALM) were included, resulting in 10 scenarios.
- EN: Variations in object geometry influence contact features (point, line, surface) during rotation, while different hand contact areas result in varying levels of tactile information. Three geometries (CUBE, CYLINDER, SQUARE PYRAMID) and two hand contact conditions (SINGLE-HAND, TWO-HAND) were selected, yielding 6 scenarios.

To ensure consistent movement speeds, each LM and CF action lasted 2 s, while EN actions lasted 4 s. Detailed conditions are shown in Figure 7.

A series of tasks were designed to evaluate the perception across different hand regions, the perceived realism of haptic experience, and object condition discrimination.

To assess perception across hand regions, after experiencing each scenario, participants were asked to mark all perceived stimulation regions on a prepared hand contour diagram and report the corresponding perceived hand regions. These regions were defined anatomically as the thenar eminence (R1), hypothenar eminence

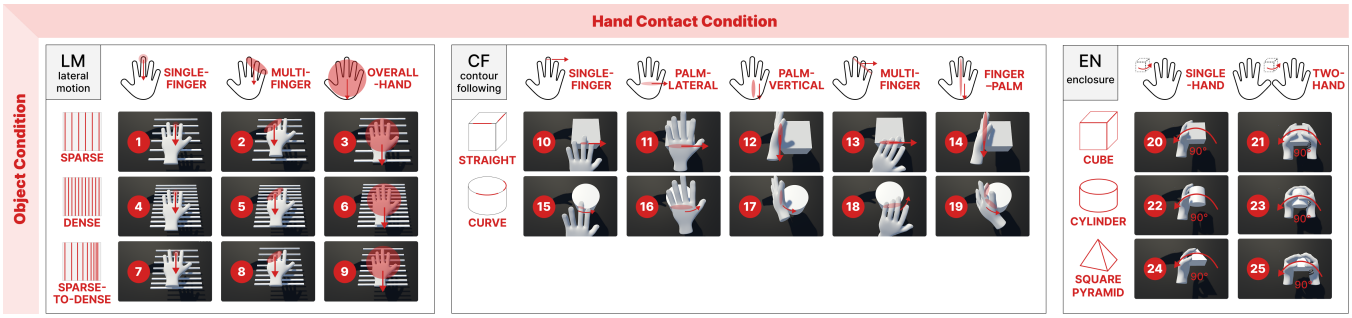


Figure 7: Conditions of Study 1.

(R2), central palm (R3), MCP joints (R4), middle fingertip (R5), ring fingertip (R6), little fingertip (R7), and finger phalanges (R8).

To evaluate perceived realism, we adopted four items from the Haptic Experience Inventory (HXI) [40] (see Appendix A) that assess how well haptic sensations simulate or represent real-world experiences. All items were rated on a 7-point Likert scale.

To examine object condition discrimination, under each EP, participants were asked to identify the corresponding object condition for each scenario using haptic feedback alone.

4.2 Participants and Procedure

We recruited 12 participants (6 male, 6 female; aged 20–29) covering several GB/T 16252–2023 hand-length categories described earlier (Section 3.1.1).

Each participant first completed a personalized mapping process (Section 3.5) linking controller contact points to virtual probes. Based on prior observations, electrodes at the MCP–finger boundary and the outer central thenar region were masked due to occasional discomfort or involuntary movements. After a brief introduction, participants then underwent a calibration procedure in which the stimulation current was increased from 50μA under randomly sampled conditions until participants reported clear and comfortable sensations, establishing an individual optimal level.

Under each EP, participants first experienced electrotactile feedback across object and hand contact conditions in random order, then marked perceived stimulation areas, reported corresponding hand regions, and rated perceived realism. After familiarization, they identified object conditions in each scenario using haptics alone. Each scenario was repeated five times with randomized order. No correctness feedback was provided during the recognition task and most participants experienced each condition at most twice. The experiment lasted approximately 100 minutes per participant.

4.3 Results and Discussion

4.3.1 Perception across hand regions. For participants' perception-region drawings, we summed per-pixel values across all participants and applied linear remapping to generate heatmaps. As shown in Figure 8, heatmaps are visualized using a viridis colormap (dark blue = low, bright yellow = high), alongside actual stimulation regions for reference. To further quantify regional perception, we fitted a generalized linear mixed-effects model (GLMM) with a binomial link, using actual stimulation and reported regional perception, with region as a fixed effect and participant as a random intercept.

Overall, the heatmaps show that participants' perceived areas generally correspond to the actual stimulation areas. From a regional perspective, perception was more stable at the fingertips, thenar eminence, and MCP joints, whereas lower consistency was observed at the proximal finger regions, hypothenar area, and central palm. This pattern was further supported by the GLMM, which revealed a significant effect of region ($\chi^2(7) = 156.17$, $p < .001$). Post hoc tests (Tukey) showed that R2 (0.75), R3 (0.62), and R8 (0.71) were significantly lower than R1 (0.94), R4 (0.94), R5 (0.97), R6 (0.95), and R7 (0.91) (all $p < .05$). These differences may be related to pressure variations during hand grip. In particular, the finger phalanges, central palm, and hypothenar regions tend to have less stable contact compared to other regions, leading to reduced perceptual reliability.

These findings indicate that participants were able to perceive variations in stimulation across hand regions, demonstrating that our electrotactile feedback can deliver tactile sensations at multiple localized hand areas, with particularly reliable perception at the fingertips, thenar eminence, and MCP joints.

4.3.2 Perceived realism. We analyzed realism ratings using linear mixed-effects models (LMMs) for each EP, with hand and object conditions as fixed effects and participant as a random intercept. Type III ANOVA with Satterthwaite approximation tested main and interaction effects, followed by Bonferroni-corrected pairwise comparisons. Bar charts are shown in Figure 9, and supplementary statistical results are provided in Appendix B.

For LM, realism ratings ranged from 4.58 to 5.62, with most scenarios exceeding 5. Participants described perceiving regularly spaced patterns (P1–P2, P9–P12) or surface irregularities (P3–P5, P7–P9, P11) or wave textures (P1, P6–P9), using analogies like "plucking guitar strings," (P2, P8, P11–P12) "grilles," (P2–P3, P9) "chopsticks," (P3–P4, P10, P12) or "bamboo mats," (P4, P7, P8). A significant main effect of object condition was observed, $F(2, 88) = 3.64$, $p = .030$, with DENSE (5.36) rated higher than SPARSE-TO-DENSE (4.90) ($p = .047$). Several participants reported that interval changes of SPARSE-TO-DENSE were less perceptible than expected (P3, P5).

For CF, realism remained at a moderate-to-high level (4.96–6.06). Participants clearly perceived object edges as "lines" moving across their hands (P1–P12), described with analogies like "a ruler" (P5, P9,

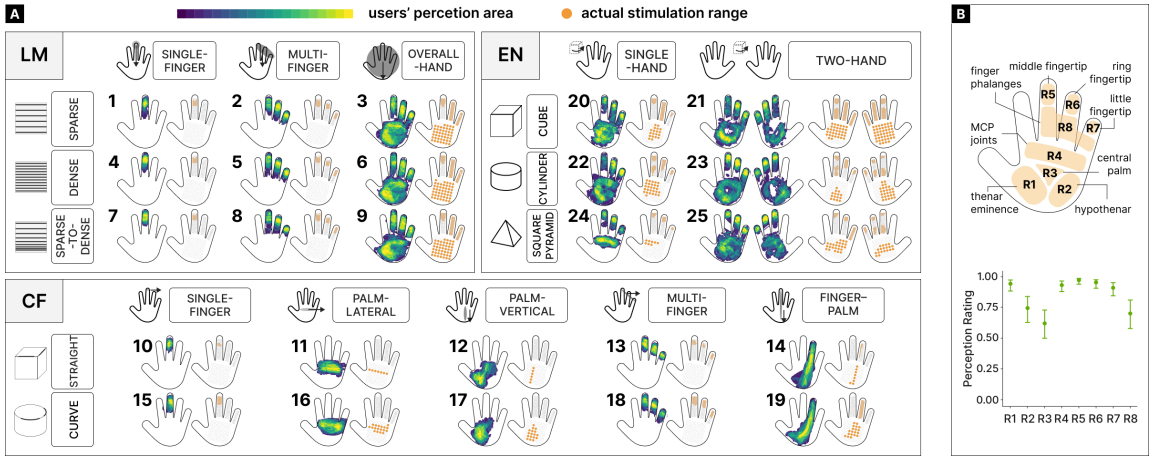


Figure 8: A, Perception Area Results. B, GLMM-estimated perception rates by region (95% CI).

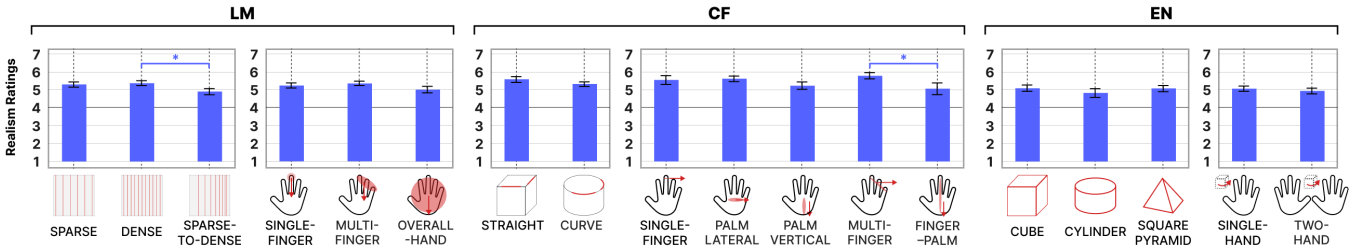


Figure 9: Perceived realism results. Bars show mean ratings; error bars indicate ±1 SE; * for $p < .05$ (Bonferroni-corrected).

P11) or "the back of a knife" (P1, P3, P7). A significant main effect of hand condition was found, $F(4, 99) = 3.40$, $p = .012$, with MULTI-FINGER (5.78) rated higher than FINGER-PALM (5.04) ($p = .019$). Some participants also noted weak sensations at the finger base and palm, which disrupted the perception of continuous edges, consistent with our findings on perception across hand regions (Section 4.3.1) and may result from regional sensitivity and lower contact pressure.

For EN, realism ratings ranged from 4.71 to 5.35. Participants reported sensing edges or vertices moving across the hands (P1–P6, P9-P11) and a sense of rotation during interactions (P2–P5, P7, P12), drawing analogies to handling everyday objects such as stone (P3, P4, P7), worn plaster models (P3, P7, P9), or earphone charging cases (P7, P9). Neither the main effects of hand condition and object condition nor their interaction were significant, all $p > .05$, suggesting relatively moderate and stable perceived realism across conditions.

Overall, these findings indicate that our electrotactile feedback achieved a moderate-to-high level of perceived realism, showing advantages in rendering fine-grained tactile properties. To further enhance realism, hand contact conditions should avoid traversing large areas with less stable perception, especially for continuous features such as edges.

4.3.3 Object condition discrimination. As shown in Figure 10, we analyzed recognition accuracy and confusion patterns under each EP using confusion matrices. To examine the effects of hand contact and object conditions, we fitted generalized linear mixed-effects models (GLMMs) with correctness as the dependent variable, hand contact and object as fixed effects, and participant as a random intercept, followed by Tukey-adjusted post hoc comparisons.

In the LM, overall recognition accuracy reached 0.80, well above chance level. SPARSE (0.85) was easier to recognize than SPARSE-TO-DENSE (0.74) ($p = .013$). Participants also reported that gradient patterns required more careful discrimination of temporal intervals (P6, P9-P10, P12). For both DENSE and SPARSE, SINGLE-FINGER performed significantly better, with higher recognition than OVERALL-HAND for DENSE textures (0.90 vs. 0.70) and than MULTI-FINGER for SPARSE (0.95 vs. 0.77) (both $p < .05$). Participants noted that SINGLE-FINGER interaction provided simpler and clearer temporal cues, facilitating the perception of pattern rhythm (P1, P3, P8).

In the CF, overall recognition accuracy increased to 0.86. STRAIGHT recognition (0.88) was slightly higher than CURVE's (0.85). Under SINGLE and MULTI-FINGER conditions, CURVE (0.83, 0.78) was recognized less accurately than STRAIGHT (0.95, 0.92) ($p = .040, .035$), which participants attributed to weaker shape variation at the fingertip without palm involvement (P1, P8, P9). For STRAIGHT, recognition was significantly lower in the PALM-VERTICAL (0.75) compared to the SINGLE-FINGER (0.95) ($p = .025$), likely due to perceptual discontinuities when stimulation crossed the palm center.

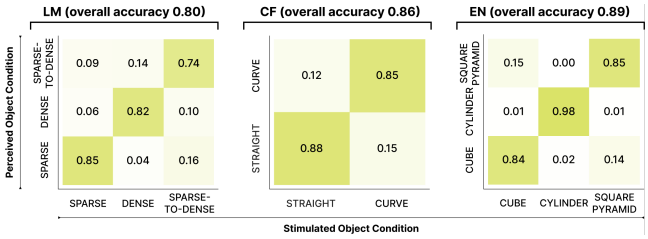


Figure 10: Confusion matrix for object condition discrimination.

In the EN, overall recognition accuracy was high (0.89). CYLINDER (0.98) was almost perfectly recognized and significantly outperformed both CUBE (0.84) (p = .004) and SQUARE PYRAMID (0.85) (p = .007), with confusions mainly occurring between CUBE and SQUARE PYRAMID. Participants reported that recognition during rotation relied on perceiving dominant geometric features across the palm, with the continuous and stable contact pattern of cylinders being easier to identify than the point- or edge-based variations of other shapes (P2, P6, P11, P12).

These results suggest that our electrotactile approach shows potential for supporting discriminable object features. In particular, some high-recognition tactile cues may support novel interaction and gameplay designs based on tactile discrimination. When further considering improvements in tactile discriminability, design implications can be derived from both object settings and hand contact settings. For object settings, gradient patterns in LM need stronger encoding contrast than non-gradient, while rotational interactions benefit from objects with clearly distinguishable geometric features, such as the point-, edge-, and surface-dominated shapes used in our study. Regarding hand contact, single-finger interaction is effective for distinguishing pattern intervals, whereas palm involvement is more suitable for edge discrimination. Notably, extensive contact in perceptually unstable regions may reduce discriminability, especially for continuous edge features in CF tasks.

5 Study 2: Evaluating the Usability of Electrotactile Method in a Simulated Gaming Environment

Study 2 extended our evaluation to a more game-like interactive environment, aiming to understand how electrotactile feedback influences both experiential quality and users' intentions to adopt the system. The study was guided by two research questions:

RQ4: How does adding electrotactile feedback, compared with purely visual feedback, affect users' enjoyment and immersion in gaming interactions?

RQ5: How does the addition of electrotactile feedback influence users' adoption intentions compared with visual-only interaction?

5.1 Study Design

In Study 2, we applied our electrotactile feedback in an item-exploration room to approximate a video game context. Building on the experimental conditions and participants' metaphorical descriptions of tactile perception from Study 1, we combined and packaged basic forms into nine game-relevant items: book, knife, wood, guitar, ruler, diamond, plant, cup, and brush. With the exception of plant (explored using LM or CF) and cup (explored using EN), all items were explored using LM, CF, and EN. The details of 24 interactions (I1-I24) are shown in Figure 11. All interaction triggers were mapped to different buttons on the gamepad. Consistent with common hand-interaction mechanics in video games, users navigated the environment using the joystick and triggered hand-object interaction animations through button presses. Each animation lasted 2–4 s to maintain comparable motion speed. To investigate the contribution of haptics beyond vision, we included two conditions (haptic vs. non-haptic), resulting in 48 total conditions (24 × 2).

Enjoyment and immersion are vital dimensions often discussed in game experience research [3]. We adopted the enjoyment subscale from the Intrinsic Motivation Inventory (Q5–Q11) [37], a measure widely used for enjoyment evaluation in Games User Research [3], and the 4-item Spatial Presence: Self-Location (SPSL) subscale from the MEC Spatial Presence Questionnaire (MEC-SPQ) [54] to evaluate immersion (Q12-Q15). All items were rated on a 7-point Likert scale.

Adoption intention was measured with two items (Q16–Q17). Participants also provided open-ended feedback on preferred gameplay contexts and improvement suggestions (Q18–Q19). The full list is provided in Appendix C.

For all haptic conditions, we additionally verified perceived realism using the same items as Study 1 to ensure that the experience met the minimum baseline; these served as validation rather than primary evaluation measures (Appendix C).

5.2 Participants and Procedure

Twelve participants (7 male, 5 female; aged 20–29) were recruited for Study 2. Their hand-length categories followed the same GB/T 16252–2023 classification used in Section 3.1.1. Ten had prior experience with game controllers. The study lasted approximately 60 minutes, was approved by the ethics committee, and all participants provided informed consent.

The personalized mapping and calibration processes are both the same as those in Study 1 (see Section 4.2). The two blocks (haptic and non-haptic) were counterbalanced, each containing 24 randomized interactions. After each trial, participants rated enjoyment and immersion (Q5–Q15); in the haptic block, they additionally completed realism items (Q1–Q4). After each block, participants reported adoption intention (Q16–Q17), followed by brief open-ended feedback (Q18–Q19).

5.3 Results and Discussion

With realism ratings for all 24 interactions remaining within or above the observed in Study 1 (see Appendix D), we proceeded to analyze enjoyment and immersion across all interactions, as well as adoption intention.

5.3.1 Enjoyment and Immersion. Enjoyment and immersion were computed as the mean scores of Q5–Q11 and Q12–Q15 respectively. For each interaction (I1–I24), paired t-tests compared haptic and non-haptic conditions, with p-values adjusted using the Benjamini–Hochberg (BH) procedure. Qualitative comments were

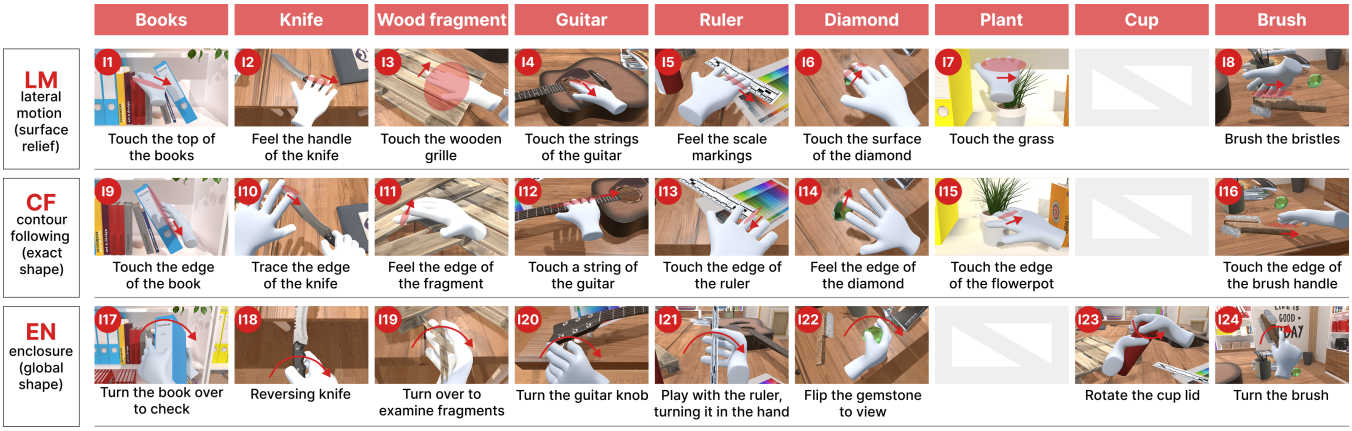


Figure 11: Interaction conditions in Study 2.

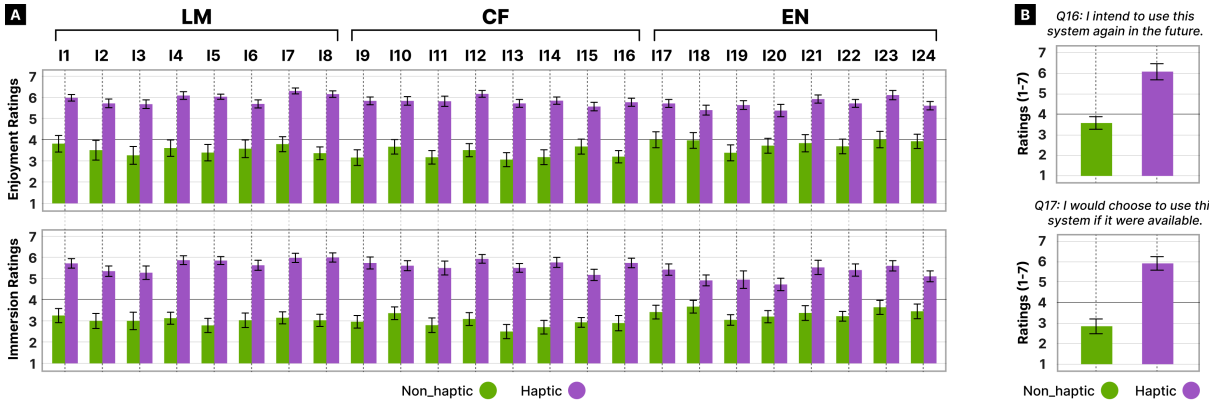


Figure 12: A, Mean scores for Enjoyment and Immersion under haptic and non-haptic conditions. Bars show mean ratings; error bars indicate ±1 SE. B, Adoption Intention scores. Bars show mean ratings; error bars indicate ±1 SE.

thematically coded by two researchers, with representative quotes selected.

Across all EPs, both enjoyment and immersion were significantly higher in the haptic condition for all 24 interactions after BH correction (all $p < .05$; see Appendix D), with mean ratings in the mid-to-high range (enjoyment: 5.30–6.27; immersion: 4.73–6.00; Figure 12). Participants noted that the added haptic feedback better conveyed object properties (P3, P9, P12), made interactions feel more engaging and surprising (P2, P6, P8, P9), and encouraged deeper exploration of the scenarios (P4, P12). These results indicate that electrotactile feedback significantly enhances enjoyment and immersion.

5.3.2 Adoption Intention. Adoption intention was compared between haptic and non-haptic conditions using paired t-tests with BH–FDR correction. Open-ended responses were thematically coded by two researchers, with representative quotes selected.

Adoption intentions were substantially higher in the haptic condition. For Q16, ratings increased from 3.58 ± 0.31 ($M \pm SE$) to 6.08 ± 0.40, $t(11) = 5.99$, $p < .001$, $d = 1.73$. For Q17, ratings increased from 2.83 ± 0.37 to 5.92 ± 0.34, $t(11) = 8.61$, $p < .001$, $d = 2.49$. As shown in Figure 12, scores rose from around 3 to nearly 6 across both items, indicating a strong positive effect of electrotactile feedback on willingness to adopt the system.

From interviews (Q25–Q26), participants envisioned diverse applications for electrotactile feedback in gaming. Many highlighted enhanced tactile detail during hand interactions, such as sensing reliefs when manipulating mechanisms (P3, P4), feeling object properties like knife edges (P3, P5), exploring environments (P2, P3, P6), petting animals (P7, P8, P12), or playing instruments (P9, P10). Others proposed gameplay extensions, including searching for items through touch (P2, P11), locating hidden objects (P2, P11, P12), and inspecting fine details in puzzle scenarios (P2, P12). A third category emphasized atmospheric and expressive effects, such as explosions (P1, P4), cutting sensations (P6, P7), magical feedback (P2, P12), and heightened tension in horror contexts (P4, P5, P11, P12). Overall, these scenarios highlight both realistic uses grounded in physical properties and expressive uses that enrich the emotional and narrative impact.

While overall feedback was positive, participants also identified areas for improvement. First, variations in sensation across hand

regions suggest the need for finer regional tuning or adaptive stimulation (P2, P3, P10). Second, the mapping and calibration workflow was described as time-consuming, and shifts in grip posture during use may introduce slight mapping drift, motivating more efficient and robust procedures (P2, P4, P6, P11). Extending electrotactile feedback to additional controller components (e.g., joysticks, buttons, triggers) could further expand interaction possibilities (P2, P5). Finally, participants noted practical considerations such as perceived safety and device portability, which are important for broader adoption (P1, P4, P6, P7, P11).

6 Limitations and Future Work

This work has several limitations that suggest directions for future research.

First, although personalized mapping and calibration enabled reliable perception, the process was time-consuming and was occasionally affected by variations in grip posture, limiting its practicality in real-world use. In our studies, as mapping was done once before the experiments, participants were asked to maintain a stable grip to minimize large pose variations. Under these instructions, no substantial perception changes or discomfort from pose shifts were observed. Future work could improve efficiency and robustness through faster automatic posture detection and adaptive, learning-based parameters optimization with minimal user input.

Second, sensation intensity was not always uniform across hand regions, and variations in stimulation range or duration occasionally led to perceptual imbalance. Addressing this through better understanding of regional sensitivity and adaptive control strategies, such as dynamic pulse adjustment, could improve consistency and comfort. Other sources of sensitivity variation, such as hand laterality, may also affect electrotactile perception and are worth further investigation.

Third, our studies aimed to investigate whether localized electrotactile cues could enable tactile sensations difficult to achieve with current gamepad haptics due to limited spatial localization, rather than comparing haptic modalities. Therefore, we did not include a direct comparison with vibrotactile feedback. Nevertheless, vibrotactile remains an important comparison target due to its widespread use in commercial gamepads. Future work could compare localized electrotactile and vibrotactile feedback using customized prototypes and further explore their respective roles and strengths in game interactions.

Fourth, for the tested motion speeds, the 33 ms contact-detection interval plus ~100 μs scan time was comparable to the reported 45 ms haptic-coordination threshold [53]. While this temporal resolution was sufficient for the tested interactions, further improving temporal resolution to support faster and more dynamic movements remains future work.

Fifth, the current prototype is not yet optimized for portability or long-term use. More compact and integrated hardware designs—for example, miniaturized HV setup, flexible control modules and improved cable routing—could enhance comfort and usability. In addition, perceived safety, adaptability to more hand shapes and usage habits, and potential impacts of electrotactile on other controller interactions (e.g., touchpad use) remain important considerations for broader adoption. Larger-scale studies should also be conducted as the prototype develops.

Finally, our evaluation focused on texture reliefs, shapes, and a limited set of hand interactions. Future work could expand tactile expressiveness by exploring a broader range of electrotactile sensations (e.g., parameter variations for roughness [2]), combining modalities such as vibration or force, and extending feedback to additional controller components (e.g., joysticks, buttons, and triggers). Exploring richer gameplay contexts, such as emotional scenarios, may further inform comprehensive design guidelines.

7 Conclusion

We presented a novel electrotactile gamepad cover and a stimulation method that delivers tactile details from virtual interactions to corresponding regions of the user's hand, supporting hand-movement interactions during gameplay. Two user studies evaluated its performance. Study 1 demonstrated that the system can reliably provide perceptible haptic cues on diverse hand regions with moderate-to-high realism, and yielded design insights for both object and hand contact settings. Study 2 extended the evaluation to game-like contexts, showing that electrotactile feedback significantly enhanced enjoyment and immersion compared to visual-only conditions. Participants also expressed strong willingness to adopt the system and offered concrete suggestions for future improvements.

Overall, our findings indicate that ElectroPad can reliably complement and extend the capabilities of current game controllers and enhance multiple dimensions of user experience, while also opening opportunities for novel forms of gameplay. With continued optimization of electrode design, stimulation methods, and long-term usability, electrotactile gamepads hold potential as a new medium for immersive and engaging interactive experiences.

Acknowledgments

We thank all the participants involved in this research and everyone who provided valuable suggestions. This research was sponsored by the National Natural Science Foundation of China (62502508, T2422027), the National Social Science Fund of China Art Project (25BG176), the Research Fund for Humanities and Social Sciences of the Ministry of Education (22YJA760082), the Fundamental and Interdisciplinary Disciplines Breakthrough Plan of the Ministry of Education of China (JYB2025XDXM122), and supported by the '111 Center' (B26063), Yuelushan Industrial Innovation Center, Lushan Lab Research Funding.

References

[1] Yahya Abbass, Strahinja Dosen, Lucia Seminara, and Maurizio Valle. 2022. Full-hand electrotactile feedback using electronic skin and matrix electrodes for high-bandwidth human–machine interfacing. *Philosophical Transactions of the Royal Society A* 380, 2228 (2022), 20210017.

[2] M Ercan Altinsoy and Sebastian Merchel. 2011. Electrotactile feedback for handheld devices with touch screen and simulation of roughness. *IEEE Transactions on Haptics* 5, 1 (2011), 6–13.

[3] Florian Brühlmann and Elisa D Mekler. 2018. Surveys in games user research. *Games user research* (2018), 141–162.

[4] Vasilije Bursać and Dragan Ivetić. 2025. A versatile tool for haptic feedback design towards enhancing user experience in virtual reality applications. *Applied Sciences* 15, 10 (2025), 5419.

[5] Cathy Fang, Yang Zhang, Matthew Dworman, and Chris Harrison. 2020. Wireality: Enabling complex tangible geometries in virtual reality with worn multi-string haptics. In *Proceedings of the 2020 CHI Conference on Human Factors in*

Computing Systems. 1–10.

[6] Michele Germani, Maura Mengoni, and Margherita Peruzzini. 2013. Electro-tactile device for material texture simulation. *The International Journal of Advanced Manufacturing Technology* 68, 9 (2013), 2185–2203.

[7] Eric J Gonzalez, Eyal Ofek, Mar Gonzalez-Franco, and Mike Sinclair. 2021. X-rings: A hand-mounted 360 shape display for grasping in virtual reality. In *The 34th annual ACM symposium on user interface software and technology*. 732–742.

[8] Daniel Groeger, Martin Feick, Anusha Withana, and Jürgen Steimle. 2019. Tactlets: Adding tactile feedback to 3D objects using custom printed controls. In *Proceedings of the 32nd annual ACM symposium on user interface software and technology*. 923–936.

[9] Chutian Jiang, Yinan Fan, Junan Xie, Emily Kuang, Kaihao Zhang, and Mingming Fan. 2024. Designing unobtrusive modulated electrotactile feedback on fingertip edge to assist blind and low vision (BLV) people in comprehending charts. In *Proceedings of the 2024 CHI Conference on Human Factors in Computing Systems*. 1–20.

[10] Arata Jingu, Nihar Sabnis, Paul Strohmeier, and Jürgen Steimle. 2024. Shaping compliance: Inducing haptic illusion of compliance in different shapes with electrotactile grains. In *Proceedings of the 2024 CHI Conference on Human Factors in Computing Systems*. 1–13.

[11] Arata Jingu, Anusha Withana, and Jürgen Steimle. 2023. Double-sided tactile interactions for grasping in virtual reality. In *Proceedings of the 36th Annual ACM Symposium on User Interface Software and Technology*. 1–11.

[12] Kurt A Kaczmarek, Mitchell E Tyler, and Paul Bach-y Rita. 1997. Pattern identification on a fingertip-scanned electrotactile display. In *Proceedings of the 19th Annual International Conference of the IEEE Engineering in Medicine and Biology Society.'Magnificent Milestones and Emerging Opportunities in Medical Engineering'(Cat. No. 97CH36136)*, Vol. 4. IEEE, 1694–1696.

[13] Hiroyuki Kajimoto. 2012. Design of cylindrical whole-hand haptic interface using electrocutaneous display. In *International Conference on Human Haptic Sensing and Touch Enabled Computer Applications*. Springer, 67–72.

[14] Hiroyuki Kajimoto. 2012. Skeletouch: transparent electro-tactile display for mobile surfaces. In *SIGGRAPH Asia 2012 emerging technologies*. 1–3.

[15] Hiroyuki Kajimoto. 2016. Electro-tactile display: principle and hardware. In *Pervasive Haptics: Science, Design, and Application*. Springer, 79–96.

[16] Hiroyuki Kajimoto, Naoki Kawakami, Susumu Tachi, and Masahiko Inami. 2004. SmartTouch: Electric skin to touch the untouchable. *IEEE computer graphics and applications* 24, 1 (2004), 36–43.

[17] Hiroyuki Kajimoto, Masaki Suzuki, and Yonezo Kanno. 2014. HamsaTouch: Tactile vision substitution with smartphone and electro-tactile display. In *CHI'14 Extended Abstracts on Human Factors in Computing Systems*. 1273–1278.

[18] Sugarragchaa Khurelbaatar, Yuriko Nakai, Ryuta Okazaki, Vibol Yem, and Hiroyuki Kajimoto. 2016. Tactile presentation to the back of a smartphone with simultaneous screen operation. In *Proceedings of the 2016 CHI Conference on Human Factors in Computing Systems*. 3717–3721.

[19] Mohammad Amin Kuhail, Jose Berengueres, Fatma Taher, and Mariam Al Kuwaiti. 2024. Exploring Haptic Technology's Role in Gaming and Entertainment. In *Advances, Applications and the Future of Haptic Technology*. Springer, 29–42.

[20] Pakkapol Lailert, Alex Gougoulaki, Hitesh Dommati, Shamin Sadrafshari, Christof Lutteroth, Cameron Steer, and Ollie Hanton. 2026. WearTactile: An Electrotactile Research Platform to Support Exploration of Nuanced Electrotactile Control for Wearable Devices. In *Proceedings of the Extended Abstracts of the 2026 CHI Conference on Human Factors in Computing Systems*. 1–6.

[21] Susan J Lederman and Roberta L Klatzky. 1987. Hand movements: A window into haptic object recognition. *Cognitive psychology* 19, 3 (1987), 342–368.

[22] Hongnan Lin, Lei Gao, Shengsheng Jiang, Hongyu Yue, Ziyi Fu, Jinyi Luo, Chengxiao Wu, Teng Han, Feng Tian, and Sriram Subramanian. 2025. Slip-Grip: An Electrotactile Method to Simulate Weight. In *Proceedings of the 2025 CHI Conference on Human Factors in Computing Systems*. 1–14.

[23] Hongnan Lin, Songxian Liu, Shengsheng Jiang, Yueyan Pang, Jian He, Teng Han, Feng Tian, and Xing-Dong Yang. 2025. ElectroClick: Enhancing Button Experiences on Surfaces with Electrotactile Sensations. *Proceedings of the ACM on Interactive, Mobile, Wearable and Ubiquitous Technologies* 9, 3 (2025), 1–26.

[24] Hongnan Lin, Xuanyou Liu, Shengsheng Jiang, Qi Wang, Ye Tao, Guanyun Wang, Wei Sun, Teng Han, and Feng Tian. 2024. Tactex: a textile interface with seamlessly-integrated electrodes for high-resolution electrotactile stimulation. In *Proceedings of the 2024 CHI Conference on Human Factors in Computing Systems*. 1–16.

[25] Weikang Lin, Dongsheng Zhang, Wang Wei Lee, Xuelong Li, Ying Hong, Qiqi Pan, Ruirui Zhang, Guoxiang Peng, Hong Z Tan, Zhengyou Zhang, et al. 2022. Super-resolution wearable electrotactile rendering system. *Science advances* 8, 36 (2022), eabp8738.

[26] Zhiming Liu, Yudong Luo, Jose Cordero, Na Zhao, and Yantao Shen. 2016. Fingereye: A wearable text reading assistive system for the blind and visually impaired. In *2016 IEEE international conference on real-time computing and robotics (RCAR)*. IEEE, 123–128.

[27] Markus Löchtefeld, Tuomas Lappalainen, Jani Väyrynen, Ashley Colley, and Jonna Häkkilä. 2017. Comparing thermal and haptic feedback mechanisms for game controllers. In *Proceedings of the 2017 CHI Conference Extended Abstracts on Human Factors in Computing Systems*. 1829–1836.

[28] Jonatan Martínez, Arturo García, Miguel Oliver, José Pascual Molina, and Pascual González. 2014. Identifying virtual 3D geometric shapes with a vibrotactile glove. *IEEE computer graphics and applications* 36, 1 (2014), 42–51.

[29] Jonatan Martínez, Arturo S García, José P Molina, Diego Martínez, and Pascual González. 2013. An empirical evaluation of different haptic feedback for shape and texture recognition. *The Visual Computer* 29, 2 (2013), 111–121.

[30] Atsushi Matsubayashi, Hiroki Oikawa, Saya Mizutani, Yasutoshi Makino, and Hiroyuki Shinoda. 2019. Display of haptic shape using ultrasound pressure distribution forming cross-sectional shape. In *2019 IEEE World Haptics Conference (WHC)*. IEEE, 419–424.

[31] Shota Nakayama, Mitsuki Manabe, Keigo Ushiyama, Masahiro Miyakami, Akifumi Takahashi, and Hiroyuki Kajimoto. 2022. Pilot study on presenting pulling sensation by electro-tactile stimulation. In *International Conference on Human Haptic Sensing and Touch Enabled Computer Applications*. Springer, 66–74.

[32] Hideaki Nishino. 2020. Introducing DualSense, the New Wireless Game Controller for PlayStation 5. *Playstation. Blog* (2020).

[33] Hiroyuki Okabe, Shogo Fukushima, Michi Sato, and Hiroyuki Kajimoto. 2011. Fingertip slip illusion with an electrocutaneous display. In *International conference on Artificial Reality and Telexistence*. 10–14.

[34] Praneeth Bimsara Perera, Ravindu Madhushan Pushpakumara, Hiroyuki Kajimoto, Arata Jingu, Jürgen Steimle, and Anusha Withana. 2025. eTactileKit: A Toolkit for Design Exploration and Rapid Prototyping of Electro-Tactile Interfaces. In *Proceedings of the 38th Annual ACM Symposium on User Interface Software and Technology*. 1–17.

[35] Mehdi Rahimi, Fang Jiang, and Yantao Shen. 2019. Non-linearity of skin properties in electrotactile applications: Identification and mitigation. *IEEE Access* 7 (2019), 169844–169852.

[36] Mehdi Rahimi and Yantao Shen. 2019. Adaptive spatial mapping of electrotactile threshold based on subdivision bio-impedance feedback. In *2019 IEEE International Conference on Real-time Computing and Robotics (RCAR)*. IEEE, 164–169.

[37] Richard M Ryan. 1982. Control and information in the intrapersonal sphere: An extension of cognitive evaluation theory. *Journal of personality and social psychology* 43, 3 (1982), 450.

[38] Mikel Sagardia, Katharina Hertkorn, Thomas Hulin, Simon Schätzle, Robin Wolff, Johannes Hummel, Janki Dodiya, and Andreas Gerndt. 2015. VR-OOS: The DLR's virtual reality simulator for telerobotic on-orbit servicing with haptic feedback. In *2015 IEEE Aerospace Conference*. IEEE, 1–17.

[39] Taiga Saito, Jianyao Zhang, Takayuki Kameoka, and Hiroyuki Kajimoto. 2021. Thermal sensation presentation to the forehead using electrical stimulation: Comparison with other tactile modalities. In *2021 IEEE World Haptics Conference (WHC)*. IEEE, 888–893.

[40] Tianzheng Shi and Oliver Schneider. 2025. Development and Initial Validation of the Haptic Experience Inventory (HXI). In *Proceedings of the 2025 CHI Conference on Human Factors in Computing Systems*. 1–21.

[41] Youngbo Aram Shim and Geehyuk Lee. 2018. Demonstrating Gamepad with Programmable Haptic Texture Analog Buttons. In *Adjunct Proceedings of the 31st Annual ACM Symposium on User Interface Software and Technology*. 194–196.

[42] Youngbo Aram Shim, Keunwoo Park, Sangyoon Lee, Jeongmin Son, Taeyun Woo, and Geehyuk Lee. 2020. FS-Pad: video game interactions using force feedback gamepad. In *Proceedings of the 33rd annual ACM symposium on user interface software and Technology*. 938–950.

[43] Bukun Son and Jaeyoung Park. 2018. Haptic feedback to the palm and fingers for improved tactile perception of large objects. In *Proceedings of the 31st annual ACM symposium on user interface software and technology*. 757–763.

[44] Yui Suga, Masahiro Miyakami, Izumi Mizoguchi, and Hiroyuki Kajimoto. 2023. 3d shape presentation by combination of force feedback and electro-tactile stimulation. In *2023 IEEE World Haptics Conference (WHC)*. IEEE, 361–367.

[45] Yui Suga, Masahiro Takeuchi, Satoshi Tanaka, and Hiroyuki Kajimoto. 2023. Softness presentation by combining electro-tactile stimulation and force feedback. *Frontiers in Virtual Reality* 4 (2023), 1133146.

[46] Taiki Takami, Taiga Saito, Takayuki Kameoka, and Hiroyuki Kajimoto. 2023. ExtEdge: Haptic Augmentation of Visual Experiences of a Smartphone by Electro-Tactile Sensation Through the Edges. In *Proceedings of the 2023 ACM Symposium on Spatial User Interaction*. 1–8.

[47] Shan-Yuan Teng, Aryan Gupta, and Pedro Lopes. 2024. Haptic permeability: Adding holes to tactile devices improves dexterity. In *Proceedings of the 2024 CHI Conference on Human Factors in Computing Systems*. 1–12.

[48] Shan-Yuan Teng, Gene SH Kim, Xuanyou Liu, and Pedro Lopes. 2025. Seeing with the hands: A sensory substitution that supports manual interactions. In *Proceedings of the 2025 CHI Conference on Human Factors in Computing Systems*. 1–15.

[49] Shan-Yuan Teng, Tzu-Sheng Kuo, Chi Wang, Chi-huan Chiang, Da-Yuan Huang, Liwei Chan, and Bing-Yu Chen. 2018. Pupop: Pop-up prop on palm for virtual reality. In *Proceedings of the 31st Annual ACM Symposium on User Interface Software and Technology*. 5–17.

[50] Hsin-Ruey Tsai, Chieh Tsai, Yu-So Liao, Yi-Ting Chiang, and Zhong-Yi Zhang. 2022. Fingerx: Rendering haptic shapes of virtual objects augmented by real objects using extendable and withdrawable supports on fingers. In *Proceedings of the 2022 CHI Conference on Human Factors in Computing Systems*. 1–14.
[51] Haruya Uematsu, Masaki Suzuki, Yonezo Kanno, and Hiroyuki Kajimoto. 2016. Tactile vision substitution with tablet and electro-tactile display. In *International Conference on Human Haptic Sensing and Touch Enabled Computer Applications*. Springer, 503–511.
[52] Myla van Wegen, Just L Herder, Rolf Adelsberger, Manuela Pastore-Wapp, Erwin EH Van Wegen, Stephan Bohlhalter, Tobias Nef, Paul Krack, and Tim Vanbellingen. 2023. An overview of wearable haptic technologies and their performance in virtual object exploration. *Sensors* 23, 3 (2023), 1563.
[53] Ingrid MLC Vogels. 2004. Detection of temporal delays in visual-haptic interfaces. *Human Factors* 46, 1 (2004), 118–134.
[54] Peter Vorderer, Werner Wirth, Feliz Gouveia, Frank Biocca, Timo Saari, Lutz Jäncke, Saskia Böcking, Holger Schramm, Andre Gysbers, Tilo Hartmann, et al. 2004. MEC spatial presence questionnaire (MEC-SPQ, English and German version): Short documentation and instructions for application. *Report to the European Community, Project Presence: MEC (IST-2001-37661)* 6 (2004), 2004.
[55] Anusha Withana, Daniel Groeger, and Jürgen Steimle. 2018. Tacttoo: A thin and feel-through tattoo for on-skin tactile output. In *Proceedings of the 31st Annual ACM Symposium on User Interface Software and Technology*. 365–378.
[56] Kuanming Yao, Jingkun Zhou, Qingyun Huang, Mengge Wu, Chun Ki Yiu, Jian Li, Xingcan Huang, Dengfeng Li, Jingyou Su, Senlin Hou, et al. 2022. Encoding of tactile information in hand via skin-integrated wireless haptic interface. *Nature Machine Intelligence* 4, 10 (2022), 893–903.
[57] Ryuhei Yokota and Katsuhiro Uchida. 2013. Information processing apparatus and control method. US Patent App. 13/724,983.
[58] Shigeo Yoshida, Yuqian Sun, and Hideaki Kuzuoka. 2020. Pocopo: Handheld pin-based shape display for haptic rendering in virtual reality. In *Proceedings of the 2020 CHI Conference on Human Factors in Computing Systems*. 1–13.
[59] Zhong-Yi Zhang, Hong-Xian Chen, Shih-Hao Wang, and Hsin-Ruey Tsai. 2022. ELAXO: Rendering Versatile Resistive force feedback for fingers grasping and twisting. In *Proceedings of the 35th Annual ACM Symposium on User Interface Software and Technology*. 1–14.
[60] Ziliang Zhou, Yicheng Yang, Jinbiao Liu, Jia Zeng, Xiaoxin Wang, and Honghai Liu. 2022. Electrotactile perception properties and its applications: A review. *IEEE transactions on haptics* 15, 3 (2022), 464–478.

A Realism Items of Study 1

Table 1: Realism Items of Study 1

Q1	The haptic sensations resembled the ones I feel in real life.
Q2	The haptic sensations closely mimicked the experiences I would expect in reality.
Q3	The haptic sensations felt familiar to real life touch.
Q4	The haptic sensations provided a true-to-life representation of real-world sensations.

B Supplementary Realism Results of Study 1

Table 2: Descriptive statistics of realism ratings (Mean ± SD) across hand contact and object conditions for each EP.

EP	Hand contact condition	Object condition	Mean ± SD
LM	OVERALL-HAND	DENSE	5.29 ± 0.92
		SPARSE	5.12 ± 1.18
		SPARSE-TO-DENSE	4.58 ± 1.20
	MULTI-FINGER	DENSE	5.62 ± 0.60
		SPARSE	5.46 ± 0.63
		SPARSE-TO-DENSE	4.94 ± 0.78
	SINGLE-FINGER	DENSE	5.17 ± 0.93
		SPARSE	5.33 ± 0.84
		SPARSE-TO-DENSE	5.17 ± 0.97
CF	FINGER–PALM	STRAIGHT	5.12 ± 1.74
		CURVE	4.96 ± 1.46
	MULTI-FINGER	STRAIGHT	6.06 ± 0.40
		CURVE	5.50 ± 1.04
	PALM-LATERAL	STRAIGHT	5.90 ± 0.59
		CURVE	5.35 ± 0.93
	PALM-VERTICAL	STRAIGHT	5.21 ± 1.33
		CURVE	5.27 ± 0.67
	SINGLE-FINGER	STRAIGHT	5.60 ± 1.49
		CURVE	5.54 ± 0.95
EN	SINGLE-HAND	CUBE	5.35 ± 0.66
		CYLINDER	4.71 ± 1.31
		SQUARE PYRAMID	5.10 ± 0.84
	TWO-HAND	CUBE	4.81 ± 1.04
		CYLINDER	4.94 ± 1.23
		SQUARE PYRAMID	5.04 ± 0.98

Table 3: Results of Type III ANOVA from linear mixed-effects models (LMM) for each EP. Degrees of freedom were estimated using the Satterthwaite approximation.

EP	Effect	F	p
LM	Hand contact condition	$F(2, 88) = 1.68$	.192
	Object condition	$F(2, 88) = 3.64$	.030*
	Interaction	$F(4, 88) = 0.76$	.552
CF	Hand contact condition	$F(4, 99) = 3.40$	.012*
	Object condition	$F(1, 99) = 3.00$	.086
	Interaction	$F(4, 99) = 0.75$	.562
EN	Hand contact condition	$F(1, 55) = 0.48$	.493
	Object condition	$F(2, 55) = 0.89$	.419
	Interaction	$F(2, 55) = 1.54$	.223

C Questionnaire Items of Study 2

Table 4 lists the questionnaire items used in Study 2.

Table 4: Questionnaire Items of Study 2

Haptic experience (Q1-Q4)	
Q1	The haptic sensations resembled the ones I feel in real life.
Q2	The haptic sensations closely mimicked the experiences I would expect in reality.
Q3	The haptic sensations felt familiar to real life touch.
Q4	The haptic sensations provided a true-to-life representation of real-world sensations.
Enjoyment (Q5–Q11)	
Q5	I enjoyed doing this activity very much.
Q6	This activity was fun to do.
Q7	I thought this was a boring activity. (R)
Q8	This activity did not hold my attention at all. (R)
Q9	I would describe this activity as very interesting.
Q10	I thought this activity was quite enjoyable.
Q11	While I was doing this activity, I was thinking about how much I enjoyed it.
Immersion (Q12–Q15)	
Q12	I felt like I was actually there in the environment of the presentation.
Q13	It was as though my true location had shifted into the environment in the presentation.
Q14	I felt as though I was physically present in the environment of the presentation.
Q15	It seemed as though I actually took part in the action of the presentation.
Adoption Intention (Q16–Q19)	
Q16	I intend to use this system again in the future.
Q17	I would choose to use this system if it were available.
Q18	What gameplay situations or scenarios would you like to experience this type of haptic feedback in?
Q19	Do you have any suggestions for improving this haptic feedback for future use?

D Supplementary Results of Study 2

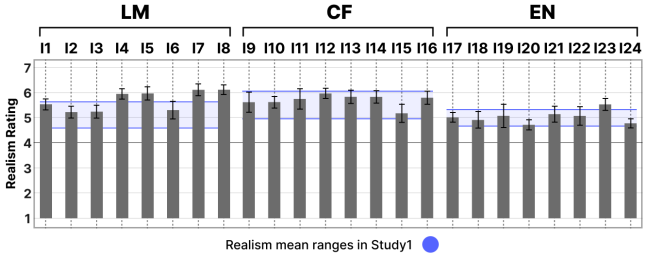


Figure 13: Haptic ratings for all 24 interactions. Bars show mean ratings; error bars indicate ±1 SE. Shaded colored bands denote the corresponding rating ranges observed in Study 1.

Table 5: Results for enjoyment

Interaction	Mean ± SD (Non-haptic)	Mean ± SD (Haptic)	p	Cohen's d	p_adj
I1	3.67 ± 1.38	5.95 ± 0.54	0.000	1.538	0.001
I2	3.36 ± 1.64	5.65 ± 0.75	0.001	1.247	0.003
I3	3.08 ± 1.48	5.61 ± 0.72	0.000	1.829	0.000
I4	3.45 ± 1.35	6.06 ± 0.70	0.000	1.470	0.001
I5	3.23 ± 1.37	6.00 ± 0.40	0.000	1.804	0.000
I6	3.40 ± 1.49	5.64 ± 0.68	0.001	1.258	0.003
I7	3.63 ± 1.25	6.27 ± 0.53	0.000	1.696	0.000
I8	3.19 ± 1.11	6.11 ± 0.62	0.000	2.335	0.000
I9	2.99 ± 1.32	5.77 ± 0.67	0.000	1.728	0.000
I10	3.52 ± 1.15	5.79 ± 0.73	0.000	1.592	0.001
I11	2.98 ± 1.12	5.76 ± 0.92	0.000	2.028	0.000
I12	3.32 ± 1.23	6.13 ± 0.60	0.000	1.759	0.000
I13	2.87 ± 1.23	5.67 ± 0.66	0.000	1.903	0.000
I14	3.00 ± 1.30	5.80 ± 0.62	0.000	1.974	0.000
I15	3.52 ± 1.28	5.49 ± 0.82	0.001	1.346	0.002
I16	3.01 ± 1.09	5.73 ± 0.64	0.000	1.969	0.000
I17	3.88 ± 1.32	5.65 ± 0.73	0.003	1.115	0.006
I18	3.83 ± 1.37	5.32 ± 0.87	0.018	0.805	0.035
I19	3.21 ± 1.33	5.58 ± 0.74	0.000	1.464	0.001
I20	3.55 ± 1.27	5.30 ± 1.04	0.001	1.329	0.002
I21	3.68 ± 1.47	5.88 ± 0.69	0.001	1.230	0.003
I22	3.54 ± 1.20	5.67 ± 0.68	0.000	1.688	0.000
I23	3.86 ± 1.44	6.07 ± 0.77	0.000	1.502	0.001
I24	3.79 ± 1.21	5.55 ± 0.76	0.001	1.344	0.002

Table 6: Results for immersion

Interaction	Mean ± SD (Non-haptic)	Mean ± SD (Haptic)	p	Cohen's d	p_adj
I1	3.27 ± 1.13	5.73 ± 0.79	0.000	1.640	0.001
I2	3.02 ± 1.21	5.35 ± 0.84	0.000	1.436	0.001
I3	3.02 ± 1.40	5.29 ± 1.05	0.000	1.599	0.001
I4	3.15 ± 0.98	5.88 ± 0.73	0.000	2.458	0.000
I5	2.79 ± 1.11	5.85 ± 0.60	0.000	2.307	0.000
I6	3.04 ± 1.18	5.65 ± 0.77	0.000	1.531	0.001
I7	3.17 ± 0.94	5.98 ± 0.74	0.000	1.842	0.000
I8	3.04 ± 1.00	6.00 ± 0.74	0.000	2.330	0.000
I9	2.98 ± 1.01	5.75 ± 0.93	0.000	1.827	0.000
I10	3.38 ± 1.05	5.62 ± 0.77	0.000	1.817	0.000
I11	2.81 ± 1.15	5.52 ± 1.10	0.000	1.895	0.000
I12	3.10 ± 1.01	5.94 ± 0.68	0.000	2.653	0.000
I13	2.50 ± 1.13	5.52 ± 0.70	0.000	1.982	0.000
I14	2.71 ± 1.13	5.77 ± 0.82	0.000	2.159	0.000
I15	2.94 ± 0.81	5.19 ± 0.89	0.000	1.586	0.001
I16	2.92 ± 1.26	5.75 ± 0.76	0.000	1.937	0.000
I17	3.44 ± 1.08	5.44 ± 0.92	0.000	1.435	0.001
I18	3.69 ± 1.06	4.92 ± 0.91	0.015	0.831	0.031
I19	3.06 ± 0.87	4.96 ± 1.47	0.005	1.009	0.010
I20	3.21 ± 0.99	4.73 ± 1.03	0.003	1.112	0.006
I21	3.40 ± 1.15	5.54 ± 1.12	0.001	1.282	0.002
I22	3.23 ± 0.76	5.42 ± 0.99	0.000	2.198	0.000
I23	3.67 ± 1.10	5.62 ± 0.79	0.000	1.658	0.001
I24	3.48 ± 1.14	5.12 ± 0.88	0.000	1.511	0.001